Design and Optimization of Spray Unit Holder and Shaft Assembly of a Linear Motor Operated Spray Gun

[1]A.K.M. Parvez Iqbal, [2]Ishak Aris, [1]M.M. Rahman and [2]Norhisam Misron
[1]Department of Mechanical Engineering, College of Engineering,
Universiti Tenaga Nasional (UNITEN), Jalan Ikram-Uniten, 43000 Kajang,
[2]Department of Electrical Engineering, Faculty of Engineering,
Universiti Putra Malaysia (UPM), 43400 UPM Serdang, Selangor, Malaysia

Abstract: In order to reduce the labor and production cost, linear motor operated automatic spray gun has been designed and developed. This spray gun consists of 2 spray units, spray unit holder and shaft assembly an air control and supply unit and a triggering unit to carry out the multiple spray operations. This study focuses on the design optimization and fabrication of the spray unit holder and shaft assembly. There are 2 links to this holder and they are 90° apart from each other. One end of the holder links are used to hold the spray units and the other ends are attached with a shaft. The shaft is kept in position in the spray gun body by the adjusting lever and can rotate 90° to either side. Due to this rotation, the position of spray units can be adjusted during the desired spray operation. Since, the highly pressurized fluid is passed through the spray unit, a high force is subjected to the end of the holder where the spray unit is held and the holder behaves like a cantilever beam. Meanwhile, the shaft is subjected to the bending moment and the torque due to the fluid pressure and the weight of the spray unit, respectively. After analyzing, dimensions and material selection have been optimized in order to fabricate the spray unit holder and shaft assembly. During the performance test, it is observed that the fabricated spray unit holder and shaft assembly can support the spray operation without any deflection and failure.

Key words: Spray gun, spray process, spray unit holder, shaft, failure analysis, deflection analysis

INTRODUCTION

Sprays can be implemented in different industrial areas such as production or process, treatment, coating, combustion, etc. In production industries, sprays can be used for drying to produce dairy products, tea, coffee, starch, pharmaceuticals, soaps and detergents. Sprays can be utilized for cooling and boiling purposes. Suspended waste liquors can be drained out using sprays. Some physical treatments can be carried out using spraying such as evaporation, ventilation, humidification, air and gas washing, industrial washing and cleaning. The coating process widely uses sprays for surface treatment, painting, insulation and undercoating materials. Multi component resins can be processed using sprays. Automobile industries and furniture industries, also use sprays for coating purposes. Particle coating and encapsulation are also carried out using sprays. Combustion is one of the areas where sprays play a major role to ignite fuel. Oil burners, diesel engines, gas turbines and rocket engines use the spray method for ignition.

Sprays can also be used in the agriculture industry to spray insecticides, herbicides and fertilizer solutions (Lefebvre, 1989). A lot of research is being conducted in relation to nozzle size prediction, optimization of flow patterns, determination of paint thickness, ergonomic studies of spray guns, etc.

The 2 Valve Covered Orifice (VCO) injectors with cylindrical and tapered nozzle holes were used to investigate the effect of nozzle hole geometry on non-evaporating diesel spray at high pressure injection. During the injection period, the oscillation in the micro-spray angle of the tapered nozzle was smaller than that of the cylindrical nozzle hole. The velocity and size of a droplet downstream with tapered nozzle hole were slower and smaller than the velocity and size of the cylindrical nozzle hole (Kong and Bae, 2012). Meanwhile Markus and Fritsching (2004), analyzed the growth of deposits in spray forming with multiple atomizers. In this research, 2 overlapping sprays were involved. The mass flux and enthalpy distribution were examined for different spray conditions and overlapping angles of the sprays.

Corresponding Author: A.K.M. Parvez Iqbal, Department of Mechanical Engineering, College of Engineering,
Universiti Tenaga Nasional (UNITEN), Jalan Ikram-Uniten, 43000 Kajang, Selangor, Malaysia

Normally for large billets in industrial production, 2 free fall atomizers are used mainly because of the increased yield (Nasr *et al.*, 2002). The effects of the rotational speed of rotary atomizer and cross-flow velocity of air on the droplet sizes were studied. Each of the 2 variables influenced the droplet size differently in a certain cross-flow velocity region. Form this study, 3 distinct spray regimes were identified according to the weber number based on orifice diameter; rotation dominant, intermediate and cross flow dominant (Choi *et al.*, 2012). Another research was carried out by Nonnenmacher and Piesche (2000) to design a hollow cone pressure swirl nozzle which could atomize newtonian fluids. In this study, they developed calculation models to foretell the drop size that depends on the hollow cone nozzle's geometry and volume flow for atomization of newtonian fluids. A new spray/wall interaction model for diesel spray was developed by Zhang. The Premixed Charged Compression Ignition (PCCI) engine relevant conditions were considered for this study. The new model implies the difference between dry wall and wetted wall for a description of the complicated spray/wall interaction process (Zhang *et al.*, 2014). In addition, atomization characteristics on the surface of a round liquid jet were investigated by Mayer and Branam (2004). Liquid atomization quality is an important parameter of many technological processes, such as in defining engine performance. This research investigates the jet performance for the single injector element to establish the influence of the injection conditions on a round liquid jet. Dynamics and atomization of a liquid film was investigated experimentally using spinning disk. In this process, a radially spreading thin liquid film which is mostly wavy was created on the surface of a spinning disk due to the centrifugal forces. The obtained drop size distribution of this study shows a bio-modal distribution for low liquid mass flow rate (Freystein *et al.*, 2013). A Coanda assisted Spray Manipulation (CSM) coller was retrofitted to a Praxair SG-100 plasma spray gun in order to change the direction of the plasma jet and powder without moving the gun at supersonic configuration. The collar designed for small vector angle could modify the trajectory of zirconia powder up to several degrees with increasing the temperature and velocity of powder. On the other hand, large angle device was capable of vectoring the plasma jet up to 45° and the powder velocity and temperature decreased steadily with vector angle (Allen and Smith, 2009; Marbey *et al.*, 2011). Flame spraying method was used to deposit titanium alloy powders and bioactive glass for fabricating composite porous coatings that can be used in bone fixation implants. Bioactive glass titanium

alloy powder blended and deposited in various weight fractions under 2 sets of spray conditions which produced different levels of porosity. After characterizing the coating, hydroxyapatite was found on the bioactive glass-alloy composite coatings that may increase the bioactivity of the coating through enhanced surface mineralization (Beherei *et al.*, 2009; Nelson *et al.*, 2011; Rakngarm *et al.*, 2008). Furthermore, a unified spray forming model used to predict the shape of the billet geometry had been developed. The developed model for atomization and the deposition processes have been joined together to get a new unified description of the spray forming process. The developed model can be used for predicting the contour and the temperature of a spray-formed billet (Hattle and Pryds, 2004). Additionally, the CFD analysis for the electrostatic powder coating process with the corona spray gun has been carried out. This research found that the final spray pattern shape and the increase of transfer efficiency depended on the space charge (Ye *et al.*, 2002). Meanwhile, a test air induction nozzle was designed and manufactured to examine design parameters impact on the characteristics of the spray and how the spray characteristics influence the flow profile (Ellis *et al.*, 2002). The interaction between air and liquid in the breakup zone of twin fluid atomization was investigated. The research was carried out by injecting the air with and without liquid (Shavit, 2001).

From the earlier discussion, it can be concluded that there are still some areas on spray guns to improve their functionality. From that point of view, a linear motor operated multiple spray operations spray gun has been designed and developed (Iqbal *et al.*, 2008, 2011a, b, 2013). This study focuses only the design of the spray unit holder and shaft assembly, the analysis and optimization of the spray unit holder and shaft assembly and their fabrication.

MATERIALS AND METHODS

Referring to Fig. 1 of the spray unit holder, shaft and spray unit assembly is comprised of 2 spray units, holder and a shaft. There are 2 links to this holder and they are 90° apart from each other. One end of the holder links are held by the spray units and the other ends are attached with a shaft. The shaft is kept in position in the spray gun body by the adjusting lever and can rotate 90° to either side. This rotation is provided to the shaft, so that the position of the spray unit can be adjusted during the desired spray operation. The adjusting lever is attached to the end of the shaft and can be locked with the gun casing after setting the proper spray position. The 3 tubes are attached with the spray unit to provide the required amount of air.
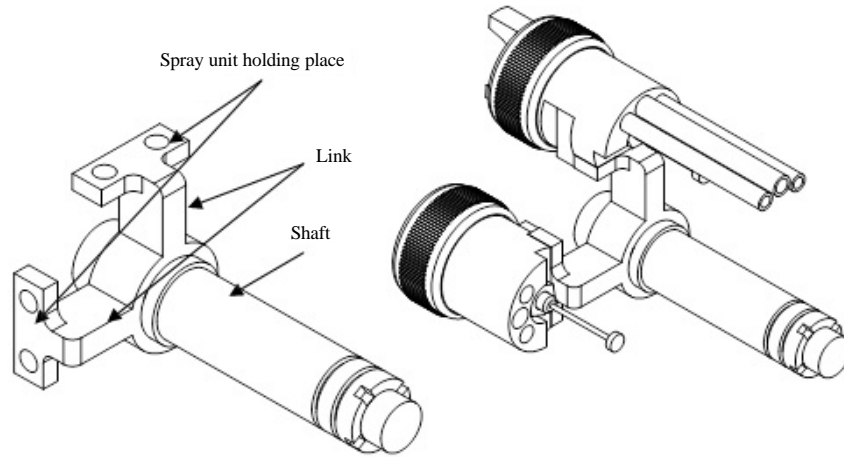
Fig. 1: Spray unit holder and shaft assembly

Analysis of spray unit holder: The spray unit holder was designed in such a way that it can hold the spray unit to the body of the spray gun. One end of the holder is used to hold the spray unit and the other end is attached to a shaft. Since, the highly pressurized fluid is passed through the spray unit, a high force is subjected to the end of the holder where the spray unit is held and the holder behaves like a cantilever beam. The main analysis of this design was to select a suitable material, beam cross-section and the best dimensions that can hold the spray unit safely with minimum deflection (Hamrok *et al.*, 2006; Hibbeler, 2005; Jalaludeen, 2000; Sigley and Mischke, 2003). The total force acting on the end of the holder was evaluated from the internal pressure of the spray housing. Equation 1 can be used to determine the total force acting on the end of the holder:

$$F = \pi r_i^2 p_i \qquad (1)$$

In order to commence the analysis of the spray unit holder, it was considered that the holder was a rectangular uniform cross-section and behaved like a cantilever beam.

The maximum stresses due to the bending and maximum shear stress within this loading condition were needed to evaluate and select the suitable material. The maximum bending stress and the maximum shear stress can be determined from the following Eq. 2 and 3:

$$\text{Maximum stress}, \sigma_{max} = \frac{Mc}{I} \qquad (2)$$

Where:
σ_{max} = The maximum normal stress in the member which occurs at a point on the cross-sectional area furthest away from the neutral axis
M = The resultant internal moment, determined from the method of sections and equation of equilibrium

I = The moment of inertia of the cross-sectional area computed about the neutral axis
c = The perpendicular distance from the neural axis to a point farthest from the neutral axis

$$\text{Maximum shear stress for the rectangular cross-section}, \tau_{max} = \frac{3V}{2A} \qquad (3)$$

Where:
V = The shear force
A = The cross-sectional area

Deflection was the major concern in this design and a minimum or no deflection of the holder is required to hold the spray unit accurately. Therefore, the Young modulus and tensile strength played a major role when selecting the materials. The allowable tensile stresses of the selected materials must be more than the calculated value using Eq. 2 and 3. For optimization in selecting the material among the selected materials; the deflection comparison should be carried out. Since, the system behaves like a cantilever beam, the Eq. 4 can provide the deflection:
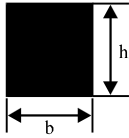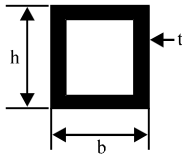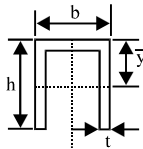
$$y = \frac{Fx^2}{6EI}(x - 3l) \qquad (4)$$

Where:
F = The force acting on the beam (N)
l = The length of the beam (m)
x = The variable length which can be vary from 0-l m

Selection of cross-section of the holder: After selecting the materials, it was necessary to investigate which cross-sectional area would provide the minimum deflection for the selected material. Since, the Young modulus is constant for all cross-sectional areas of the selected material, only the change of moment of

Table 1: Cross-sectional areas and their moment of inertia

Type of cross-section	Figures	Moment of inertia I
Solid rectangular		$I = \dfrac{1}{12}bh^3$
Shell type rectangular		$I = \dfrac{1}{12}b \times h^3 - \dfrac{1}{12}(b-2t) \times (h-2t)^3$
Channel type		$I = \left[\dfrac{1}{12}(b-2t) \times (t)^3 + (b-2t) \times t\left(\overline{y} - \dfrac{t}{2}\right)^2 \right]$ $+ 2\left[\dfrac{1}{12}t \times h^3 + (t \times h)\left(\dfrac{h}{2} - \overline{y}\right)^2 \right]$

inertia can provide the different deflection. About 3 cross-sections were chosen for this analysis. They were solid rectangular, shell type rectangular and the channel shape cross-section. Table 1 shows the different cross-sectional areas and the governing equations to evaluate the moment of inertial.

Since, the different cross-sections provided a different moment of inertia, the deflection is also different. Among these 3 cross-sectional areas, 1 cross-section was selected which can provide the minimum deflection. From the mentioned earlier analysis material, the cross-sectional area and dimension of the holder were determined. After getting all of the required data from the analysis, it was necessary to satisfy the safety condition which is stated that:

$$\sigma_{allow} \geq \frac{M_{max}c}{I}$$

And:

$$\tau_{allow} \geq \frac{3V}{2A}$$

Where:
σ_{allow} = Allowable stress = Tensile stress/Factor safety
τ_{allow} = Allowable shear stress

Analysis of the shaft: The shaft of the spray gun was attached to the spray unit holder. Therefore, it was subjected to the bending moment and the torque. The bending moment results from the fluid pressure and the torque results from the weight of the spray unit. Since, the shaft was directly attached to a holder, it would be more cost effective if the same material could be used for

fabrication. Using the distortion energy theory, the minimum diameter of the shaft was obtained where the failure will first start as expressed in Eq. 5:

$$d = \left(\frac{32n_s}{\pi\sigma_y} \sqrt{M^2 + \frac{3}{4}T^2} \right)^{\frac{1}{3}} \quad (5)$$

Where:
d = The diameter of the shaft (m)
σ_y = The yield strength of the shaft material (N m^{-2})
n_s = The factor of safety
M = The moment due to the bending
T = The torque due to the torsion

Due to the use of ductile materials for analysis, maximum shear stress theory and maximum distortion energy theory can be the optimum choice to predict the failure. According to these theories, failure can be protected if the following criteria are followed; for maximum shear stress theory:

$$|\sigma_1| \leq \sigma_y, \quad |\sigma_2| \leq \sigma_y \quad (6)$$

σ_1, σ_2 have the same signs;

$$|\sigma_1 - \sigma_2| \leq \sigma_y \quad (7)$$

σ_1, σ_2 have opposite signs. For maximum distortion energy theory:

$$\left(\sigma_1^2 - \sigma_1\sigma_2 + \sigma_2^2 \right) \leq \sigma_y^2 \quad (8)$$

Where:

σ_1 = The maximum principal stress
σ_2 = The minimum principal stress
σ_y = The design yield stress

Effect of fatigue in shaft analysis: Since, the spray unit was directly attached to the shaft, there was a chance to fluctuate the load due to the bending and torsion. Therefore, fatigue should be considered when calculating the diameter of the shaft. For the fatigue condition, the maximum shear stress theory is expressed in Eq. 9:

$$d = \left[\frac{32n_s}{\pi S_y} \sqrt{\left(M_m + \frac{S_y}{S_e} K_f M_a \right)^2 + \left(T_m + \frac{S_y}{S_e} K_{fs} T_a \right)^2} \right]^{\frac{1}{3}} \quad (9)$$

Where:

S_y = The yield stress
S_e = The endurance limit
M_m = The mean bending moment
M_a = The alternating bending moment
K_f = The bending fatigue stress concentration factor
T_m = The mean torque
T_a = The alternating torque
K_{fs} = The shear fatigue stress concentration factor

For reversed bending and steady torsion $M_m = 0$ and $T_a = 0$, therefore the Eq. 9 becomes to Eq. 10:

$$d = \left[\frac{32n_s}{\pi S_y} \sqrt{\left(\frac{S_y}{S_e} K_f M_a \right)^2 + \left(T_m \right)^2} \right]^{\frac{1}{3}} \quad (10)$$

RESULTS AND DISCUSSION

The holder was 27 mm long and to start the analysis, it was considered that the holder was a rectangular uniform cross-section with (10×6 mm) dimension and behaves like a cantilever beam. After calculating the bending and shear stress, materials for spray unit holder were selected. Table 2 shows the calculated values of maximum moment, maximum shear, moment of inertia, bending stress, shear stress and the selected materials. Determination of bending and shear stress play an

important role in material selection process. Because in order to avoid the failure, allowable stress of selected material must be more than the calculated value.

Selection of material of spray unit holder: Since, deflection is the major concern of this design and the minimum deflection of the holder is required to perform the spray unit accurately, therefore to select the suitable material between these 2 materials deflection comparison should be carried out. Figure 2 shows the deflection of the selected materials of spray unit holder when the corresponding length of the holder was varied.

From the graphical presentation shown in Fig. 2, it is clear that the steel (ultra-high strength) provides less deflection than the steel alloy 4340. Therefore, steel (ultra-high strength) can be the best choice for the design of spray unit holder.

Selection of cross-section of spray unit holder: Since, the material had already been chosen, it was now necessary to investigate which cross-sectional area would provide the minimum deflection for the selected material. About 3 cross-sections were chosen such as solid rectangular cross-section, shell type cross-section and channel type for this analysis.

From Fig. 3, it is clear that the rectangular solid cross-section provides the minimum deflection among these 3 cross-sections. Therefore, the rectangular solid cross-section was selected for the holder.
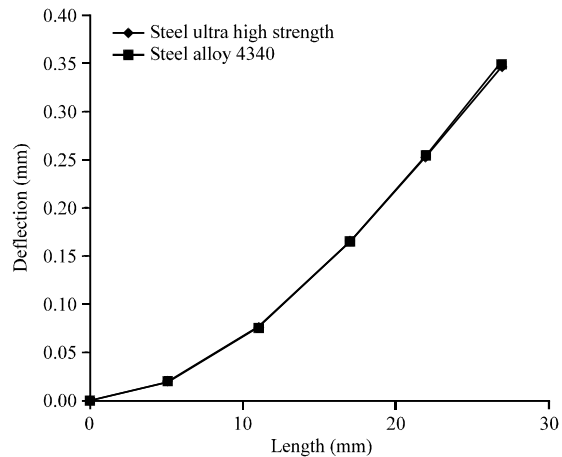

Fig. 2: Length corresponding deflection

Table 2: Bending, shear stress and selected materials

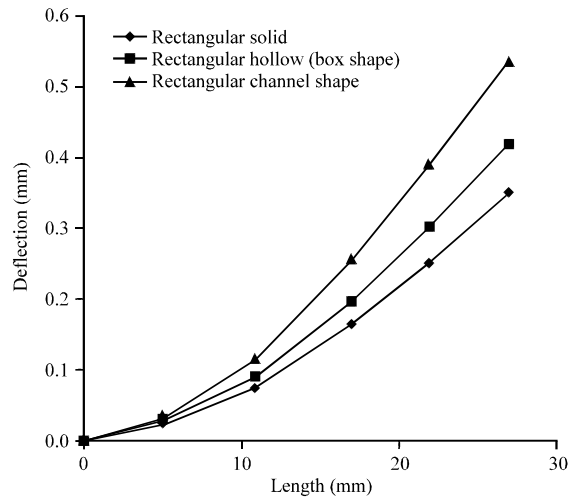| Maximum moment (M_{max} in kNm)	Maximum shear (V in kN)	Moment of inertia (I in m^4)	σ_{max} (kPa)	τ_{max} (kPa)	Selected materials
0.1485	5.5	5×10^{-10} m^4	1485000	137500	Steel (ultra-high strength), steel alloy 4340 (oil-quenched and tempered)

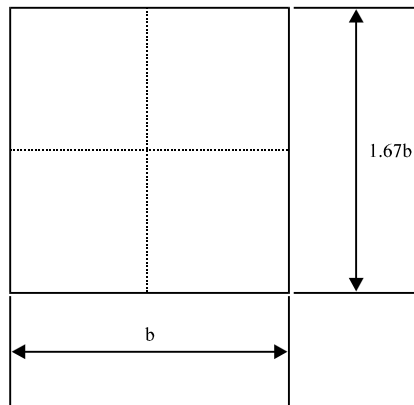Fig. 3: Length corresponding deflection of different cross-sections

Fig. 4: Cross-sectional area

From the earlier analysis, it can be concluded that the holder may be fabricated from steel ultra high strength material with a rectangular cross-section (6 mm width, 10 mm height and 27 mm length). Before finishing the analysis it was needed to satisfy the safety condition. Steel ultra-high strength has the tensile strength of 2000 MPa. The factor of safety 2 was selected. Therefore, the allowable stress is 1000 MPa and the allowable shear stress is 500 MPa. From the calculation, it was observed that that the calculating bending stress was 1485 MPa which is more than the allowable stress. Therefore, design criterion was failed in bending. On the other hand, calculating shear stress of 137.5 MPa is less than the allowable shear stress. Therefore, design criterion was satisfied in shear. Since the bending criterion failed, it was needed to redesign on the basis of bending. Let, consider the cross-section as shown in Fig. 4 in order to evaluate the width b:

$$\sigma_{allow} = \frac{M_{max}c}{I}; \quad 1000000 = \frac{0.1485 \times 0.835b}{\frac{1}{12}b(1.67b)^3};$$

$$b = 0.00684 \text{ m} = 6.84 \text{ mm}$$

Form this calculation, it can be concluded that the new width of the cross-sectional area is $6.48 \approx 7$ mm and the height of the cross-section is $(1.67 \times 7) \approx 12$ mm. The base of the holder is a cylindrical section which is subjected to the same maximum moment of the beam. From the bending point of view, it is supposed to satisfy the bending criterion. An outside diameter of 12 mm and an inside diameter of 8 mm were obtained from the preliminary design. Following analysis is shown to evaluate the diameter of the base of the spray unit holder:

$$\sigma_{allow} \geq \frac{M_{max}c}{I}; \quad 1000000 \leq \frac{0.1485 \times 0.006}{\frac{\pi}{64}(0.012^4 - 0.008^4)};$$

$$1000000 \leq 10908233$$

Therefore, the cylindrical section should be redesigned. Let, the outside diameter of the cylindrical section is D and the inside diameter is 0.67D. From the bending criterion, it is required:

$$\sigma_{allow} = \frac{M_{max}c}{I}; \quad 1000000 = \frac{0.1485 \times 0.5D}{\frac{\pi}{64}(D^4 - 0.67D^4)};$$

$$D = 0.012375 \text{ m} = 12.375 \text{ mm}$$

Where, D is the outside diameter of the base of the spray unit holder. The inside diameter is of 8.28 mm.

Analysis result of the shaft: The shaft of the spray gun was attached to the spray unit holder. Therefore, it was subjected to bending moment and the torque. The bending moment results from the fluid pressure and the torque results from the weight of the spray unit. Since, the shaft was directly attached to a holder, it would be cost effective if the same material could be used for fabrication. Maximum bending moment of 187.0176 Nm and maximum torque of 0.32 Nm were used to evaluate the minimum diameter of the shaft of 13.35 mm. According to the distortion energy theory, from this diameter, failure would be started; therefore it is necessary to verify this diameter using the distortion energy theory and the maximum shear stress theory. By using these to failure theories minimum safe diameter of the shaft would be evaluated. Table 3 shows the diameters and their corresponding failure status.

Table 3: Diameter of the shaft and its corresponding status using failure theories

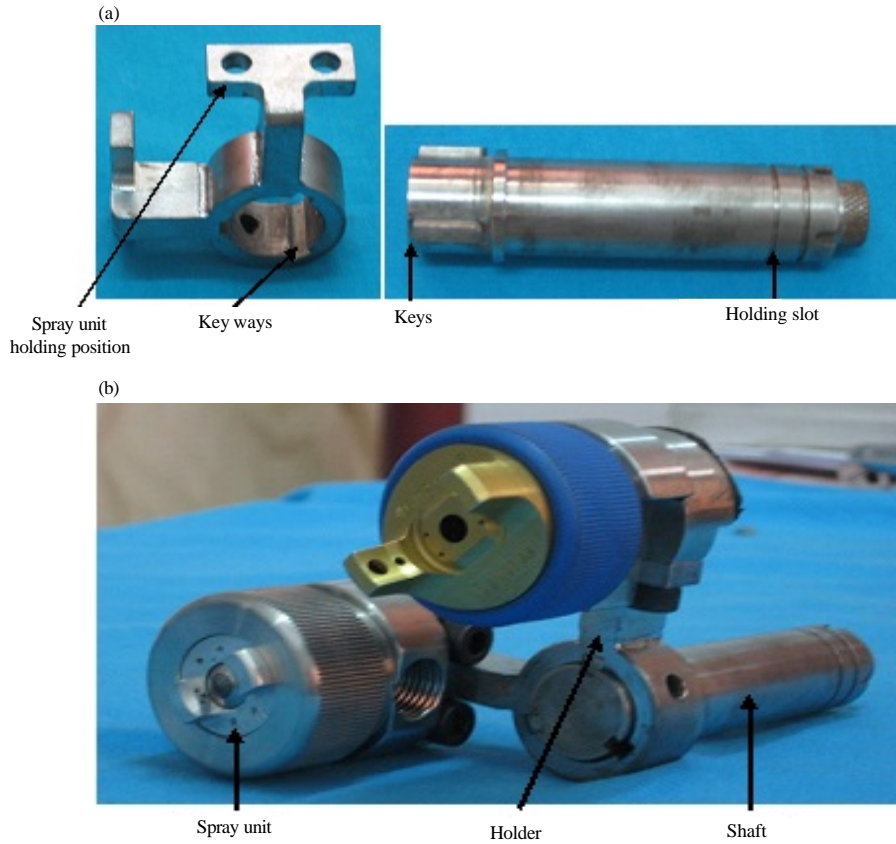| Diameter (mm)	σ_1 (N m^{-2})	σ_2 (N m^{-2})	Max shear stress theory $\lvert\sigma_1-\sigma_2\rvert\leq\lvert\sigma_1\rvert$	Max distortion energy theory ($\sigma_1^2-\sigma_1-\sigma_2+\sigma_2^2$)$\leq\sigma_y^2$	Status
13.35	809.707×10^6	-592.7	809.70×10^6≥800×10^6	6.55×10^{17}≥6.4×10^{17}	Fail
13.5	774.2506×10^6	-566.7	774.25×10^6≤800×10^6	5.99×10^{17}≤6.4×10^{17}	Safe

Fig. 5: a) Holder and shaft of the spray system; b) Holder and shaft assembly of the spray system

Therefore, the safe minimum diameter of the shaft is 13.5 mm for this loading condition. Since the spray unit is directly attached to the shaft, fluctuation of load may exert on the shaft due to the high pressurized fluid that flows through the spray unit. Therefore, fatigue should be considered to calculate the diameter of the shaft. After considering the fatigue, the safe minimum diameter of the shaft was evaluated and it was 19 mm.

Fabrication of spray unit holder and shaft assembly: The spray unit holder, shaft and their assemblies are shown in Fig. 5. The welding, drilling and milling operations were carried out to fabricate the holder. The welding was used to develop the structure of the holder; meanwhile the milling operation was carried out to generate the key-ways inside the ring of the holder. Using these key-ways the holder would be attached firmly to the shaft. The

2 threaded holes were, also provided at the periphery of the ring of the holder to protect the sliding tendency of the holder during the spray operation. At the upper part of the holder, 2 holes were provided according to the design to insert the bolt to grip the spray unit to the holder. A 19 mm shaft was manufactured using a lathe machine and a milling machine. The lathe machine was used to provide the proper cylindrical shape to make a slot around the periphery of the shaft to wear the C-clip and to perform the knurling operation at the end of the shaft. The milling operation was carried out to fabricate the key-ways at the front part of the shaft to keep the holder in the proper position. The holder and shaft, both were made of mild steel, though in the design, it was mentioned as harden steel because of the availability of material in the local market and its cost. An epoxy coating was used to protect the components from rusting.

CONCLUSION

This study has discussed the complete design and analysis of the spray unit holder and shaft assembly of a linear motor operated multiple spray operations spray gun. CATIA software has been used to develop the model of the spray unit holder and the shaft. The spray unit holder has been considered as a cantilever beam, therefore beam deflection theory has been used to obtain suitable materials and cross-sectional area of the spray unit holder. Failure theories for static loading condition (distortion energy theory and maximum shear stress theory) have been used to obtain the diameter of the shaft. Fatigue effect has been considered to finalize the diameter of the shaft. Finally, spray unit holder and shaft assembly have been fabricated according to the design and tested their performance.

ACKNOWLEDGEMENTS

REFERENCES

Allen, D. and L.B. Smith, 2009. Axisymmetric coanda-assisted vectoring. Exp. Fluids, 46: 55-64.

Beherei, H.H., R.K. Mohamed and T.G. El-Bassyouni, 2009. Fabrication and characterization of bioactive glass(45S5)/Titania biocomposites. Ceram. Int., 35: 1991-1997.

Choi, M.S., S. Yun, J.H. Jeong and A. Corber, 2012. Spray in cross flow of a rotary atomizer. Atomization Sprays, 22: 143-161.

Ellis, M.C.B., T. Swan, P.C.H. Miller, S. Waddelow, A. Bradley and C.R. Tuck, 2002. PM-Power and Machinery: Design factors affecting spray characteristics and drift performance of air induction nozzles. Biosyst. Eng., 182: 289-296.

Freystein, M., T. Borsdorf, T.G. Roisman and P. Stephan, 2013. Experimental investigation of dynamics and atomization of a liquid film flowing over a spinning disk. Atomization Sprays, 23: 589-603.

Hamrok, J.B., S.R. Schmid and B.O. Jacobson, 2006. Fundamental of Machine Elements. 3rd Edn., McGraw Hill, New York, pp: 235-250.

Hattle, J.H. and N.H. Pryds, 2004. A unified spray forming model for the prediction of billet shape geometry. Acta Materialia, 52: 5275-5288.

Hibbeler, R.C., 2005. Mechanics of Materials. 6th Edn., Prentice Hall, New York, pp: 185-228.

Iqbal, A.K.M.P., I. Aris and N. Misron, 2008. Design and development of a slot-less permanent magnet linear motor using permeance analysis method for spray application. Int. J. Applied Electromagn. Mech., 43: 365-378.

Iqbal, A.K.M.P., I. Aris, N. Misron, M.H. Marhaban and W. Asrar, 2011a. Thrust analysis and measurement of a tubular linear permanent magnet motor in spray application. J. Japan Soc. Applied Electromagn. Mech., 19: S83-S86.

Iqbal, A.K.M.P., I. Aris, N. Misron, M.H. Marhaban and W. Asrar, 2011b. Design process involved in developing mechanism of linear motor operated multiple spray operations spray gun. Austr. J. Basic Applied Sci., 5: 843-850.

Iqbal, A.K.M.P., I. Aris, M.M. Rahman and N. Misron, 2013. Design and optimization of the housing of spray unit of a linear motor operated spray gun. Indian J. Sci. Technol., 6: 5167-5175.

Jalaludeen, S.M., 2000. Machine Design. Anuradha Agencies, Kanpur, India, pp: 31-45.

Kong, J. and C. Bae, 2012. Effect of nozzle hole geometry on non-evaporating diesel spray characteristics at high-pressure injection. Atomization Sprays, 22: 1-21.

Lefebvre, A.H., 1989. Atomization and Sprays. Hemisphere Publishing Corporation, New York, pp: 18-24.

Marbey, K., L.B. Smith, G. Whichard and T. McKechnie, 2011. Coanda-assisted spray manipulation collar for a commercial spray gun. J. Thermal Spray Technol., 20: 782-790.

Markus, S. and C.C.U. Fritsching, 2004. Analysis of deposit growth in spray forming with multiple atomizers. Mater. Sci. Eng. A, 383: 166-174.

Mayer, W.O.H. and R. Branam, 2004. Atomization characteristics on the surface of a round liquid jet. Exp. Fluids, 36: 528-539.

Nasr, G.G., A.J. Yule and L. Bending, 2002. Industrial Sprays and Atomization. Springer Verlag, New York, pp: 35-64.

Nelson, M.G., A.J. Nychka and G.A. McDonald, 2011. Flame spray deposition on titanium alloy bioactive glass composite coatings. J. Thermal Spray Technol., 20: 1339-1351.

Nonnenmacher, S. and M. Piesche, 2000. Design of hollow cone pressure swirl nozzle to atomize Newtonian Fluids. Chem. Eng. Sci., 55: 4339-4348.

Rakngarm, A., Y. Miyashita and Y. Mutoh, 2008. Formation of hydroxyapatite layer on bioactive Ti and Ti-6A1-4V by simple chemical technique. J. Mater. Sci. Mater. Med., 19: 1953-1961.

Shavit, U., 2001. Gas-liquid interaction in the liquid breakup region of twin fluid atomization. Exp. Fluids, 31: 550-557.

Sigley, J.E. and C.R. Mischke, 2003. Mechanical Engineering Design. 6th Edn., McGraw Hill, New York, pp: 178-200.

Ye, Q., T. Steigleder, A. Scheibe and J. Domnick, 2002. Numerical simulation of the electrostatic powder coating process with a corona spray gun. J. Electrostat., 54: 189-205.

Zhang, Y., M. Jia, H. Liu, M. Xie, T. Wang and L. Zhou, 2014. Development of a new spray/wall interaction model for diesel spray under PCCI-engine relevant conditions. Atomization Sprays, 24: 41-80.